

See discussions, stats, and author profiles for this publication at: <https://www.researchgate.net/publication/231231154>

Capping Agent Assisted and Ag-Catalyzed Growth of Ni Nanoflowers

ARTICLE *in* CRYSTAL GROWTH & DESIGN · AUGUST 2010

Impact Factor: 4.89 · DOI: 10.1021/cg100740e

CITATIONS

21

READS

43

4 AUTHORS, INCLUDING:



Samarpita Senapati

IIT Kharagpur

7 PUBLICATIONS 81 CITATIONS

[SEE PROFILE](#)



Suneel Srivastava

IIT Kharagpur

90 PUBLICATIONS 1,661 CITATIONS

[SEE PROFILE](#)



Koushik Biswas

IIT Kharagpur

57 PUBLICATIONS 420 CITATIONS

[SEE PROFILE](#)

Capping Agent Assisted and Ag-Catalyzed Growth of Ni Nanoflowers

S. Senapati,[†] S. K. Srivastava,^{*,†} S. B. Singh,[‡] and K. Biswas[‡]

[†]Department of Chemistry and [‡]Department of Metallurgical and Materials Engineering,
Indian Institute of Technology, Kharagpur-721302, India

Received June 3, 2010; Revised Manuscript Received July 26, 2010

ABSTRACT: Capping agent (triethanolamine (TEA), diethanolamine (DEA), ethylene glycol (EG)) assisted silver-catalyzed nickel particles with flowerlike morphology has been synthesized using nickel(II) chloride hexahydrate as a precursor and hydrazine hydrate as a reducing agent by simple heating at 60 °C for 10 min. X-ray diffraction studies confirmed that the synthesized nickel is highly crystalline with face centered cubic structure. Field emission scanning electron microscopy (FESEM) and transmission electron microscopy (TEM) images revealed the formation of a nickel nanoflower irrespective of the capping agent used. High resolution transmission electron microscopy (HRTEM) of the single petal obtained in the presence of TEA shows that the fringes are equispaced with a lattice separation of 0.203 nm corresponding to the (111) plane of the fcc nickel. When the same reaction is performed at 40 and 80 °C, cauliflower-like morphology of the nickel nanoparticles and horn spheres of nickel are formed respectively. A mechanism has been proposed for the growth of nickel nanoparticles with the progress of the reaction based on scanning electron microscopy (SEM) and TEM. The nickel nanoparticles exhibit ferromagnetic behavior with the remnant magnetization being maximum using DEA as the capping agent in comparison to the values reported so far in the literature.

1. Introduction

Because of the small size and high surface area to volume ratio, metal nanoparticles often exhibit interesting optical, electronic, magnetic, and chemical properties that differ considerably from their bulk counterparts.^{1–3} In this regard, magnetic nanoparticles have received a considerable amount of attention because of their interesting applications as magnetic fluids,⁴ memory storage,⁵ biomedical applications,^{6,7} and catalysis.⁸ Nickel nanoparticles are one such important type of material, which have attracted much attention due to their uses in numerous practical applications, for example, in magnetic sensors,⁹ fuel cells,¹⁰ conducting materials,¹¹ solid phase heterogeneous catalysis,¹² and biomolecular separation.⁶ Ni can also be used as a fine substitute for noble metal Pd or Pd/Ag used in the internal electrodes of multilayer ceramic capacitors (MLCCs).¹³ It is also well established that the properties of nanomaterials are controlled by their morphologies and structures.¹⁴ Therefore, it is necessary to develop various approaches to prepare high-quality nickel nanoparticles. The most successful methods to prepare monodispersed nickel nanoparticles involve the wet chemical reduction of nickel salt in aqueous or organic solvents as one of the facile and diverse ways to control the particle size and morphology.¹⁵ The most commonly employed reducing agents are NaBH₄^{16,17} and hydrazine hydrate.^{18–21} Ni et al.²² prepared nickel nanoflower by reduction of Ni(dmg)₂ complexes by a hydrothermal route. They also prepared nickel nanoflowers consisting of hexagonal nano-platelets.²³ Liu et al.¹⁴ synthesized sea urchin like metallic nickel nanocrystals using Ni(NO₃)₃·6H₂O in the presence of CTAB by a hydrothermal method. Wang et al.²⁴ reported the synthesis of a hierarchical nickel structure using Ni(NO₃)₂·6H₂O as a nickel salt and glycine as the complexing agent. Mathew et al.²⁵ synthesized nanoflowers by the reduction of nickel chloride

using ethanol as the solvent. In addition, very few reports are available on the synthesis of nickel nanoparticles with a spherical type of morphology using silver catalyst and in the absence of any capping agent.^{26–28} It may be interesting to mention that reduction of nickel salt by hydrazine hydrate leads to the formation of nano-sized nickel only in the presence of hydroxide.^{1,22–25}

However, until now, to the best of our knowledge, there have been no reports regarding the silver-catalyzed synthesis of nickel nanoparticles without hydroxide forced in the presence or absence of any capping agent(s). Only one report exists on Pt-catalyzed synthesis of nickel nanoparticles using hydrazine hydrate as a reducing agent without the addition of alkali.²⁹ Encouraged by this, we report for the first time, the successful synthesis of the capping agent assisted and silver-catalyzed growth of nickel nanoparticles with flowerlike morphology in the absence of alkali. It is expected that the present research work may provide new dimensions in developing Ni nanoparticles through a simple approach, which can be scaled up and further explored as a solid-phase, heterogeneous catalyst for various organic reactions.

2. Experimental Section

2.1. Materials. Nickel chloride (NiCl₂·6H₂O), hydrazine hydrate (N₂H₄·H₂O), and triethanolamine (TEA), ethylene glycol (EG), diethanolamine (DEA), and silver nitrate (AgNO₃) were purchased from E. Merck (India) Limited, Mumbai, Merck Specialties Private Limited, Mumbai, Merck Limited, Mumbai, Sisco Research Laboratories Pvt. Ltd. Mumbai, India, and Merck Limited, Worli, Mumbai, respectively. Double distilled water was used throughout the experiments.

2.2. Synthesis. At room temperature, 0.0041 mol of NiCl₂·6H₂O was taken in a beaker and dissolved in distilled water. TEA was added to this solution such that, the molar ratio was maintained as 1:1 and the resultant mixture was stirred for 30 min. Subsequently, 3 mL (0.0599 mol) of hydrazine hydrate was added to this. The greenish color of the solution initially turned bluish and ultimately to bluish-pink with the pH value maintained to about

*Author to whom correspondence should be addressed. Tel: 91-3222-283334. Fax: 91-3222-255303. E-mail: sunit@chem.iitkgp.ernet.in.

10. The entire solution was placed on a hot plate maintained at 60 °C. To this, the aqueous solution of AgNO₃ catalyst (<0.0041 mM) (molar ratio of nickel salt/silver salt ≥ 1000:1) was added and stirred. Within 10 min, the reaction mixture attained 60 °C. After another 5 min, the pink-colored solution changed to gray, and black particles were formed with clear supernatant within 10 min. These particles were found to be strongly magnetic and recovered by using a permanent magnet and washed with distilled water and dried under a vacuum at 40 °C. In the same way, magnetic Ni particles were synthesized using DEA and EG as capping agents separately keeping the molar ratio of NiCl₂·6H₂O/capping agent as mentioned above (i.e., 1:1). We have also synthesized magnetic Ni without using a capping agent and observed that black magnetic particles with a clear supernatant are formed within 20 min.

2.3. Characterization. The phase analysis of different capping agent assisted silver-catalyzed Ni was carried out using PW 1710 diffractometer, Philips, Holland, with Co K_α radiation ($\lambda = 0.179$ nm) with a scanning rate of 3° per min. The morphology of the metal particles was studied by scanning electron microscopy (SEM) on a Carl Zeiss SEM analyzer at an accelerating voltage of 20 kV and field emission scanning electron microscope (FESEM) on Carl Zeiss Supra 40 instrument at an accelerating voltage of 20 kV. The particle size of Ni nanoparticles was found using a Phillips CM 200 high resolution transmission electron microscope with an acceleration voltage of 200 kV, and digital images were taken on a Gatan multipole charge-coupled device (CCD) camera. The selected area electron diffraction (SAED) pattern was also obtained. The samples for TEM analysis were prepared by dispersing the powder product in acetone and placing a drop of the dispersion on a copper grid and drying in air at room temperature. Energy dispersive X-ray (EDX) analysis of the sample was carried out on an Oxford instrument INCA attached to the scanning electron microscope. Magnetization (M) was measured using Lakeshore Cryotronics Inca USA 7400 series Vibrating Sample magnetometer (VSM) at room temperature by varying magnetic field strength (H).

3. Results and Discussion

Our preliminary experiments have established that the basic pH (about 10) is a necessary condition in the reduction of Ni(II) to Ni(0) by hydrazine hydrate. In addition, the size of the nickel particles could be controlled by adjusting the molar ratio of the Ni precursor to hydrazine hydrate. When the molar ratio of hydrazine hydrate to NiCl₂ is ≥12, though smaller sized particles of nickel are obtained,¹ the uncontrolled growth of nickel particles in the solution leads to polydispersity.²⁹ In order to overcome this, seed-mediated synthesis has been used, which involves the addition of the salt solutions of nucleating agents, such as silver,^{27,28} platinum,^{29,30} and palladium³¹ in the reaction system. When these metal salts are reduced by the reducing agents, small metallic seeds (e.g., Ag, Pt, and Pd) are formed. These in situ generated metallic seeds act as a catalyst in promoting the reduction of nickel salt by hydrazine hydrate.²⁶ In the present work, the small silver seeds are generated in situ by hydrazine hydrate mediated reduction of silver salts, which catalyzes the reduction of NiCl₂ by remaining hydrazine hydrate and accelerates the nucleation as well as controls the size of the growing particles even in the absence of NaOH. This is also confirmed when the same reaction is carried out in the absence of silver seed, where no black precipitate is formed even after an extended duration of 2 h.

It is already reported that the addition of hydrazine hydrate to the aqueous solution of Ni²⁺ salt forms a Ni-hydrazine complex, for example, [Ni(N₂H₄)₂]Cl₂, [Ni(N₂H₄)₃]Cl₂, and [Ni(N₂H₄)₆]Cl₂.²⁹ The formation of any of these Ni-hydrazine complexes depends on the reaction temperature and the molar ratio of nickel salt to hydrazine hydrate.^{32,33} In our synthetic

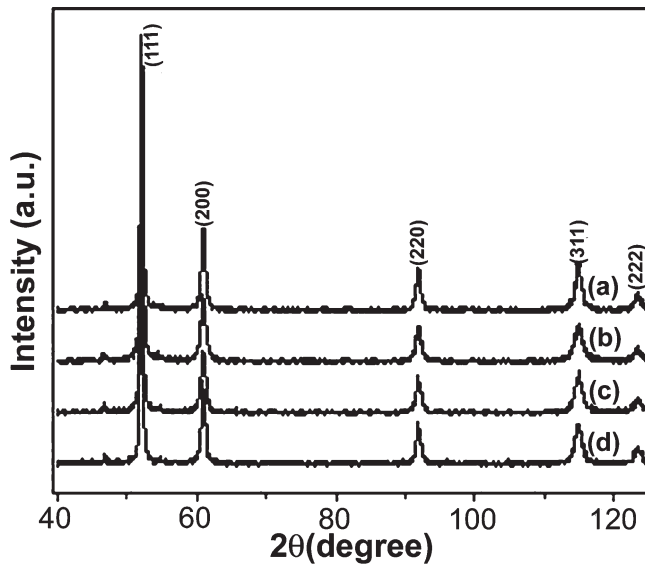


Figure 1. X-ray diffraction patterns of as-prepared nickel particles at 60 °C in the presence of different capping agents (a) TEA, (b) DEA, (c) EG, and (d) in the absence of capping agent.

procedure, we maintained the concentration of the nickel salt solution significantly low (4.1 mM) and also the molar ratio of nickel salt to hydrazine hydrate as 1:15, where it forms a bluish-pink colored stable [Ni(N₂H₄)₂]Cl₂ complex.³⁴ The black color nickel particles are formed when 4.1 × 10⁻³ mM aqueous AgNO₃ is added to the above complex solution and the reaction is carried out at 60 °C for 10 min with continuous stirring. The product so formed is found to be strongly magnetic.

It may be noted that the silver ions react with hydrazine hydrate to form H₂N-NH₂-Ag⁺ complex.³⁵ This complex in the presence of OH⁻ ions, generated from the reversible dissociation of hydrazine hydrate,³⁶ forms hydrazyl radical (·N₂H₃) and metallic silver,³⁵ which acts as a catalyst as well as a nucleating agent in the reacting system. The hydrazyl radical so formed undergoes dimerization to form tetrazane (NH₂NH-NHNH₂) as an intermediate.³⁷ The terminal amino groups of NH₂NH-NHNH₂ cleave to generate NH₃³⁷ and fulfill the prerequisite condition of the basic reaction medium responsible for the formation of nickel from Ni²⁺ in the presence of hydrazine hydrate as the reducing agent. Thus, based on this, the following mechanism for the formation of nickel has been proposed:

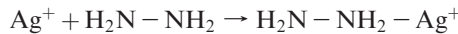
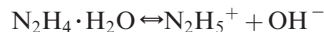


Figure 1 shows the typical X-ray diffraction (XRD) profile in the 2θ range of 40° to 125° of the synthesized nanosized magnetic nickel obtained by using silver as catalyst in the

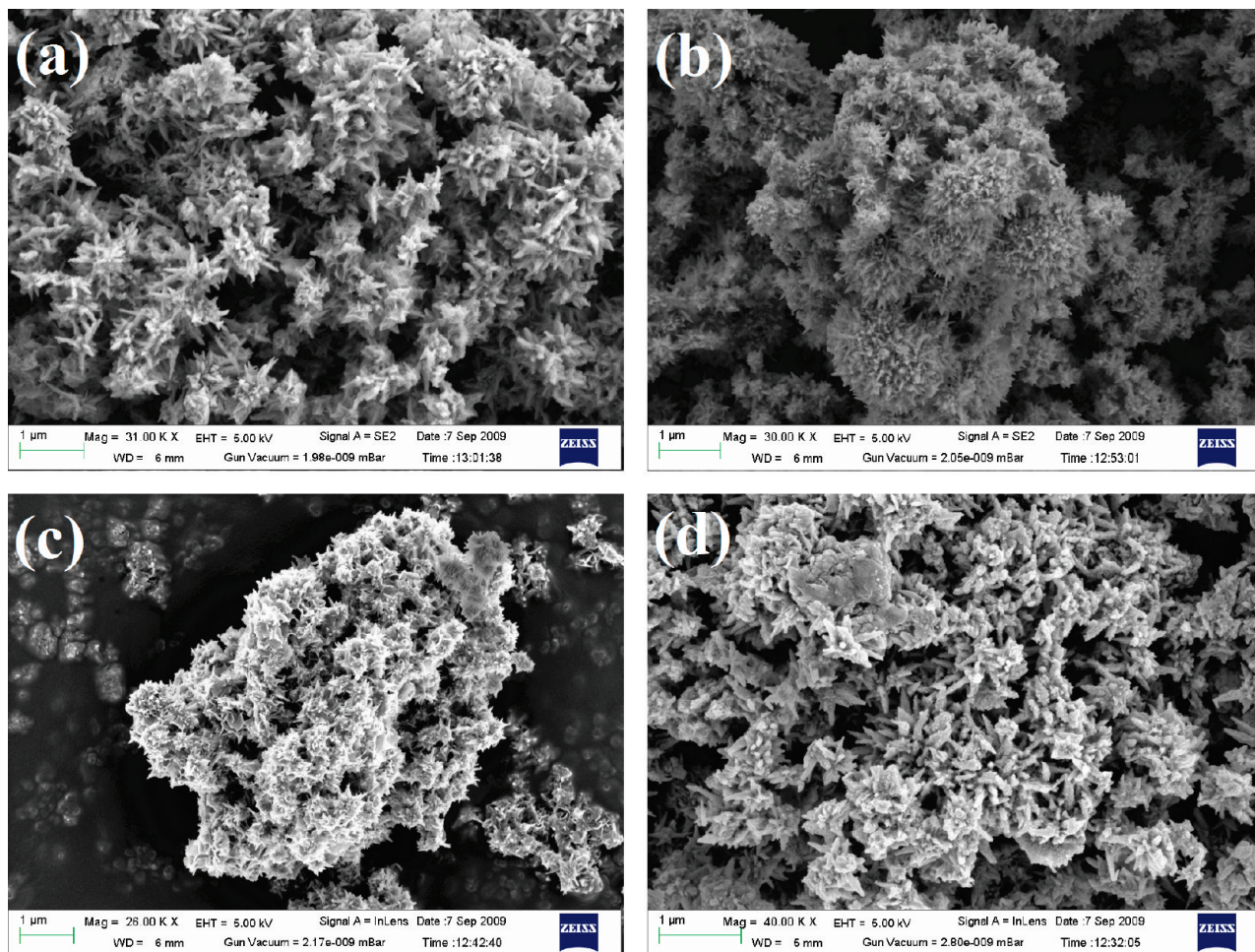


Figure 2. FESEM images of nickel particles prepared at 60 °C in the presence of capping agents (a) TEA, (b) DEA, (c) EG, and (d) in the absence of capping agent.

presence as well as in the absence of various capping agents. The diffractograms show the presence of the five characteristics peaks corresponding to $2\theta = 52.17, 61.015, 91.76, 114.93$, and 123.48° for (111), (200), (220), (311), and (222) planes, respectively, and could be indexed on the basis of face-centered cubic nickel (JCPDS card no. 04-0850). In all the XRD patterns, no peaks due to NiO , Ni_2O_3 , nor $\text{Ni}(\text{OH})_2$ as impurities are observed. This could be attributed to the fact that reaction of NiCl_2 with $\text{N}_2\text{H}_4 \cdot \text{H}_2\text{O}$ produces N_2 gas,¹ which is bubbled up continuously creating an inert atmosphere resulting in the formation of high purity nickel within the stimulated time of about 10 min at 60 °C. Thus, the introduction of an inert atmosphere from external sources is not required for the formation of high purity metallic nickel, which is otherwise necessary when the reducing agent such as sodium borohydride is used.¹⁷ It is also noted that no additional peaks of silver are present in the diffractogram. This may be possibly due to extremely smaller molar ratio of silver salt to nickel salt (1:1000), which could not be detected by XRD.²⁶ It is also observed that the magnetically recovered Ni is easily dispersed and not settled rapidly even though sonication has been put off.

It is well-known that the size and shape of the material play an important role in determining its various properties. Hence, prepared nickel has been characterized by SEM, FESEM, TEM, and HRTEM. Figure 2a–c shows the FES-EM images of Ni prepared at 60 °C for 10 min in the presence

of EG, DEA, and TEA as capping agents. It is evident from this that nickel prepared under different conditions exhibits flowerlike morphology composed of a solid core and the small conelike petals growing radially from the spherical core. The formation of such flowerlike nickel possibly consists of two steps: the formation of a solid core and subsequent growth of nanoparticles on the surface in the form of petals to form a nanoflower. In the beginning of the reaction, a certain number of nickel particles are produced on the already prepared silver seeds, and as the reduction proceeds the newly formed particles spontaneously transfer to the surface of existing particles in all directions, resulting in the formation of nanospheres, that is, the core of the flower.²⁵ It may also be mentioned that the nickel salt hydrazine complex plays a key role in the formation of the final flowerlike structure.³⁸ Because of the formation of this complex, the concentration of free Ni^{2+} ion is sharply reduced; hence rate of the reaction is slowed down due to the lower concentration of nickel ions available for the formation of Ni. As a result, the continuous additions of nickel particles occur on the circumferential edges because these edges have higher free energies²⁴ and form the spiky surface. These spikes act as seeds for the further growth of the nanocones,³⁹ which form the petals of the final product. The FESEM image in Figure 2d shows that the Ni particles when prepared without using any capping agents also possess flowerlike morphology.

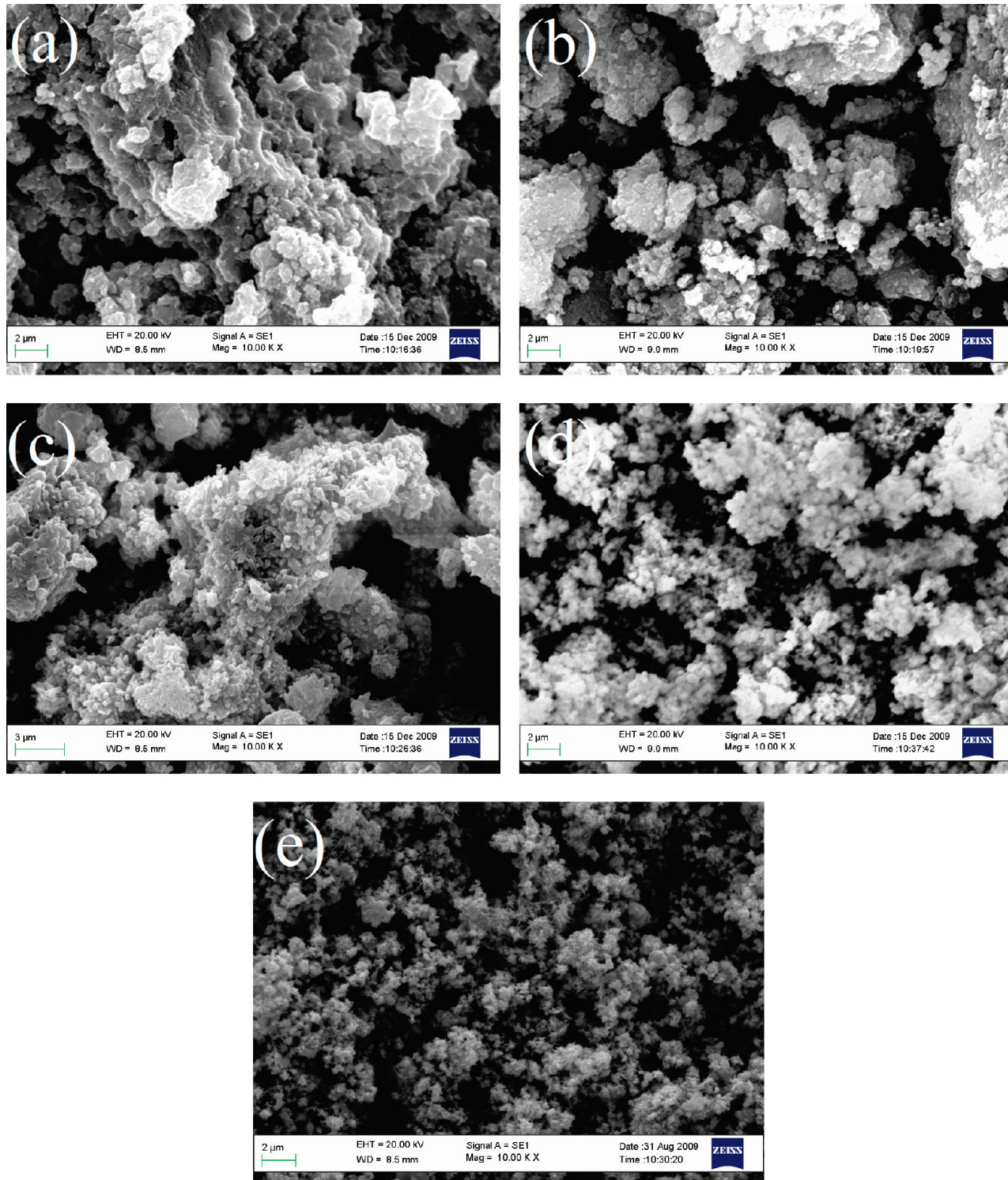


Figure 3. SEM images of the product obtained by adding hydrazine hydrate to the aqueous NiCl_2 and TEA solution at (a) room temperature, and thereafter heating this reaction at $60\text{ }^\circ\text{C}$ for (b) 5 min, (c) 7 min, (d) 8 min, and (e) 10 min.

The above mechanism is also confirmed by the addition of hydrazine hydrate to aqueous AgNO_3 and NiCl_2 solution in the presence of TEA at room temperature and is followed by heating to attain $60\text{ }^\circ\text{C}$ in 10 min. Subsequently, the morphology of products obtained at this moment of addition and thereafter heating for 5, 7, 8, and 10 min has been analyzed by SEM and findings are shown in Figure 3. The EDX spectrum of the product obtained at the point of addition of hydrazine hydrate at room temperature shows the presence of the peaks

due to Ni, Cl, N, and O. However, after heating with an increase of the reaction time, from 5 to 8 min, the peaks due to Cl and N tend to disappear and the intensity of the Ni peak begins to increase. When the duration of the reaction is maintained for 10 min, nickel is the only detected element, in addition to a small peak due to oxygen possibly due to the aerial oxidation of the nickel and is irrespective of the capping agents used. The presence of such oxygen peaks during the synthesis of nickel is not unusual and has also been noticed in

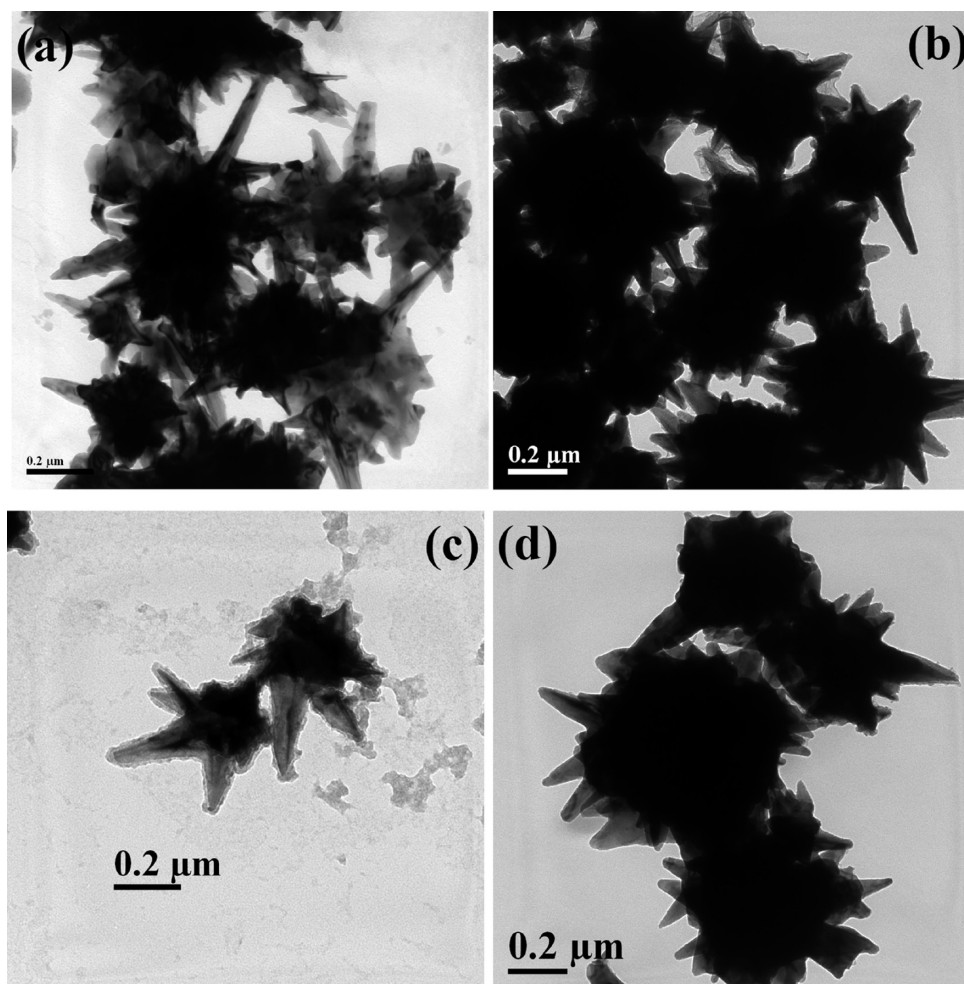


Figure 4. TEM images of nickel prepared at 60 °C in the presence of (a) TEA, (b) DEA, (c) EG, and (d) in the absence of capping agent.

the EDX analysis by others.^{25,30} It can also be noted that the presence of nickel oxide due to aerial oxidation of nickel could not be detected by XRD owing to the very small amount in the product. Figure 3 shows the SEM images of the starting materials and the product formed at different times of reaction. This SEM study of the product after 5 min of the reaction shows the irregular morphology. After 7 and 8 min, some spiky surfaces are formed due to the formation of more nickel particles obtained by the silver catalyzed reduction of nickel hydrazine complex. After the completion of the reaction (10 min), flowerlike particles are formed. It is also observed that even after sonicating for 30 min, this nanostructure remains more or less intact as confirmed from the TEM in Figure 4a–d. This confirms the formation of nanoflowers with its petals assembled at the center, agreeing well with the findings based on SEM. TEM studies clearly show that the nickel nanoflowers prepared in the presence of TEA have a diameter of 40–60 nm and a length of 90–150 nm. In the presence of DEA as capping agent, diameter and length are 50–90 nm and 130–190 nm, respectively, whereas in EG these dimensions are 95–110 nm and 170–280 nm, respectively. But in the absence of any capping agents, the length and diameter are in the range of 130–250 nm and 250–350 nm, respectively, which are relatively much larger compared to values in the presence of capping agents. HRTEM studies have also been used to investigate more details about the morphology of the flowerlike structure for TEA capped

product. Figure 5a shows the HRTEM image of a single petal revealing the cone shape of the petal with sharp edges. The magnified view of the part of this petal in Figure 5b clearly indicates that the lattice planes are very well aligned in a parallel manner without any noticeable defects with the interlayer distance of 0.203 nm. This matched well with the *d*-value in XRD of the fcc lattice nickel corresponding to the separation of the (111) planes. SAED pattern of the petals in Figure 5c also confirms the presence of the (111) plane of Ni. TEM images in Figure 6 shows that nearly cauliflower and horn sphere like nickel particles are developed, when, the reaction is carried out at 40 and 80 °C, respectively, in the presence of TEA used as a capping agent. Figure 7 shows the FESEM images of the product formed at different temperatures in the presence of TEA as the capping agent. It is essential to point that the reaction when carried out at 40 °C takes nearly 30 min to be completed. At higher temperature (80 °C) horn sphere like nickel nanoparticles are formed instead of the flower because at a given concentration of the reactants there is a temperature limit for the formation of a nanoflower. When this limit is exceeded, the particles form because of the faster reducing rate.²⁵

The room temperature magnetic properties of the Ni nanoparticles prepared in the absence of any capping agent and in the presence of different capping agents have been studied, and the corresponding magnetization curves are displayed in Figure 8a–d. M-H hysteresis loops are observed

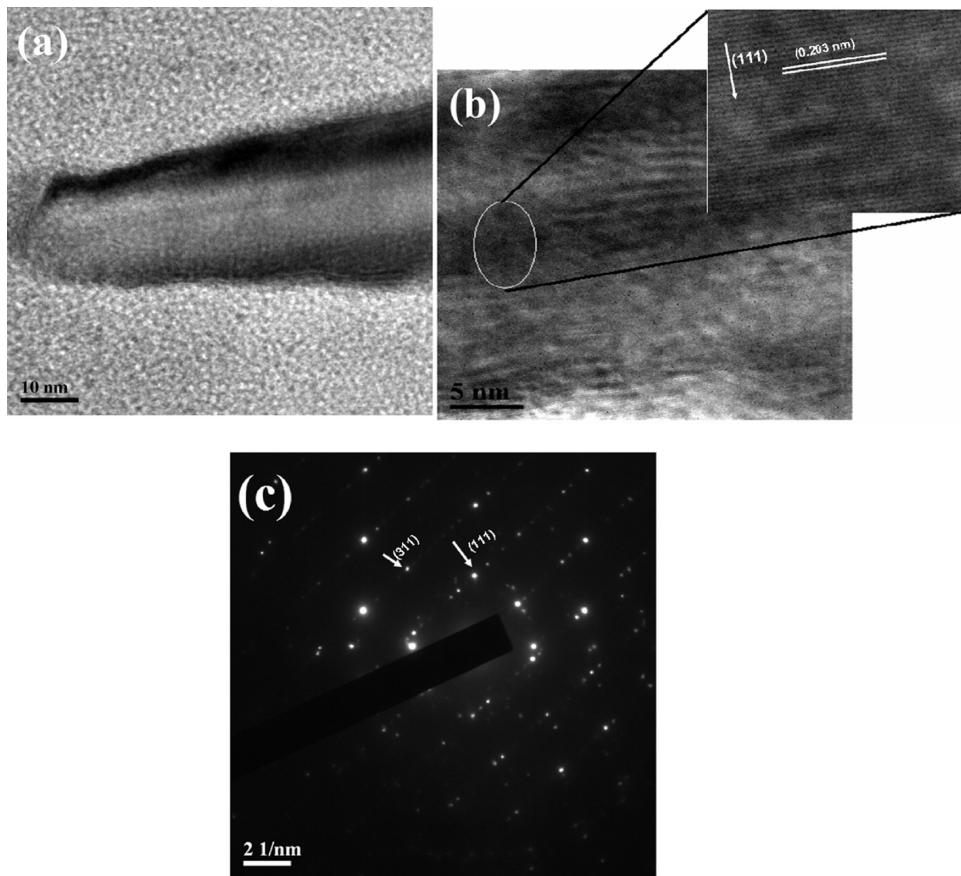


Figure 5. (a) TEM image of a single petal, (b) HRTEM image, and (c) SAED pattern of the single petal in the product obtained at 60 °C in the presence of TEA.

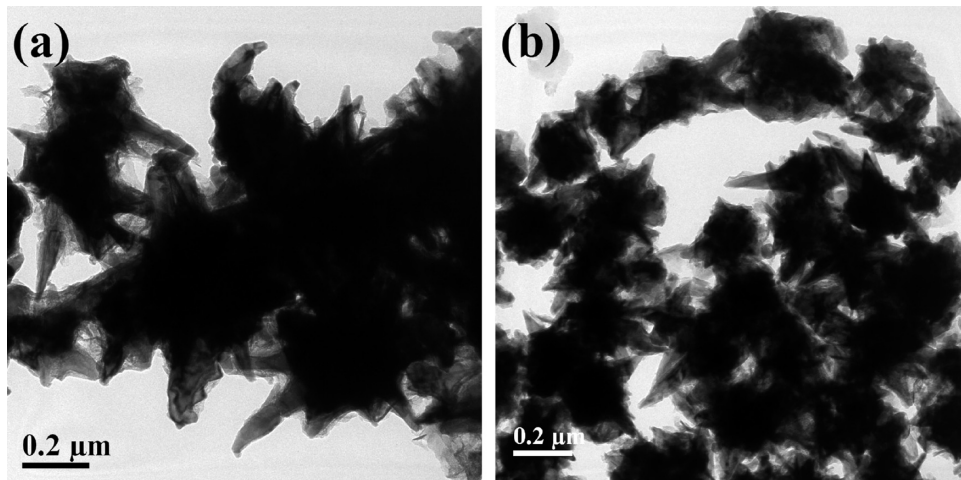


Figure 6. TEM images of nickel prepared by using TEA as the capping agent at (a) 40 °C and (b) 80 °C.

in all the cases, irrespective of the manner in which nickel has been synthesized. Table 1 records the coercivity (H_c), saturation magnetization (M_s), and remnant magnetization (M_r) values for nickel particles when synthesized using TEA, DEA, and EG capping agents and also in the absence of any capping agent. This clearly demonstrates that the H_c values of nickel nanoflowers prepared either in the presence or absence of capping agents in our case are relatively more enhanced in comparison to the bulk metal ($H_c = 10$ Oe, $M_s = 55$ emu/g, and $M_r = 2.7$ emu/g) and may be attributed to the small size and shape anisotropy.^{40–43} In

addition, there is a possibility that the increase in surface area and the magnetic interaction between the petals in the nickel nanoflowers may reduce the total magnetic moment at a given field resulting in a lower M_s value in comparison to the bulk nickel.^{44–46} The comparison of M_r values of the Ni nanoparticles of varying morphologies, for example, sphere, wire, flower, urchinlike, hierarchical with our prepared nickel nanoparticles of flowerlike morphology shows that it is relatively much lower when nickel is prepared using TEA and EG as the capping agent. On the other hand, the improvement in M_r value in our work is maximum for

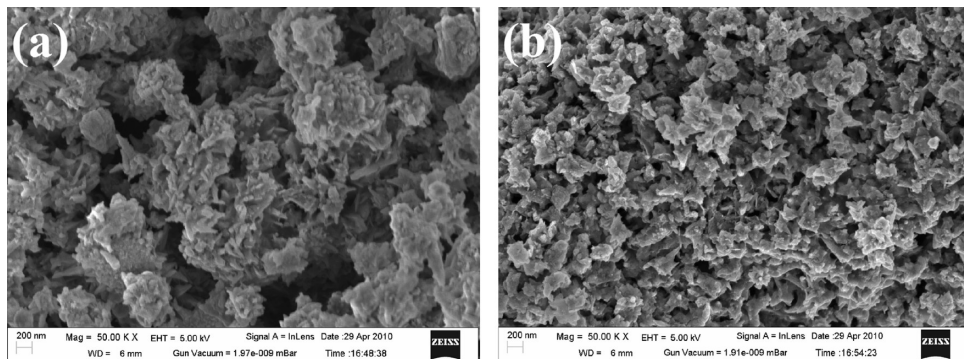


Figure 7. FESEM images of nickel at different temperatures (a) 40 °C and (b) 80 °C.

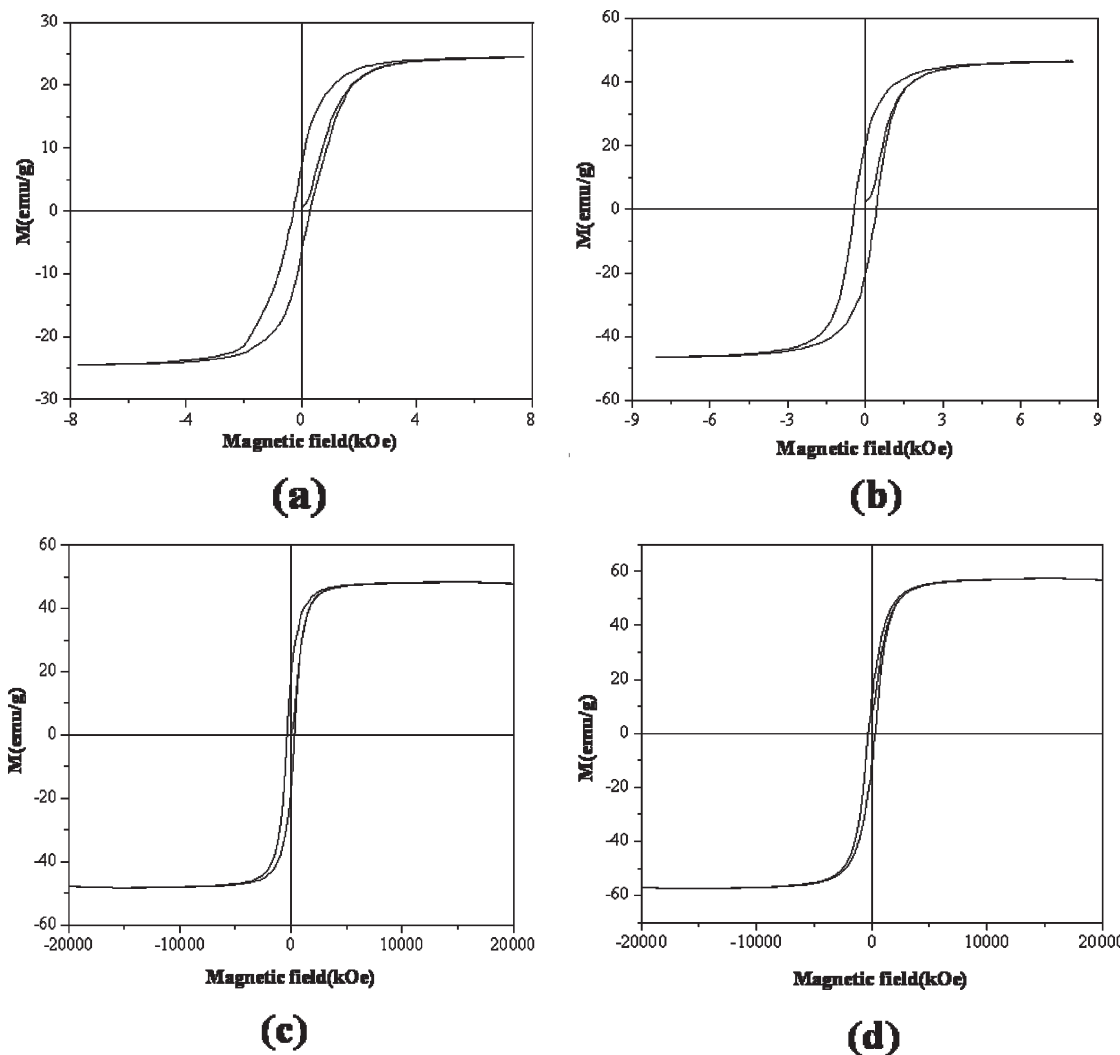


Figure 8. Magnetization study of nickel nanoflower prepared at 60 °C in the presence of capping agents (a) TEA, (b) DEA, (c) EG, and (d) in the absence of any capping agent.

Table 1. Coercivity (H_c), Saturation Magnetization (M_s), and Remnant Magnetization (M_r) Values for Nickel Particles When Synthesized Using TEA, DEA, and EG Capping Agents and Also in the Absence of Any Capping Agent

capping agent used	M_s (emu g ⁻¹)	M_r (emu g ⁻¹)	H_c (Oe)
TEA	29.8	1.143	259.44
DEA	46.5	20.10	404
EG	48.55	1.512	322
no capping agent	56.45	12.86	275

nickel nanoparticles obtained by DEA capping, and this M_r value is also comparable when nickel nanoparticles are prepared without using any capping agent. Interestingly, this value is also found to improve by 40% in the presence of DEA compared with the already reported nanosized nickel with flowerlike^{22,25,47,48} and other types of morphologies,^{24,49–52} suggesting thereby its future potential applications in high density recording media.⁴⁹

4. Conclusions

The catalytic activity of Ag seeds can be used for the seeded growth and time saving reduction of nickel salt by hydrazine hydrate in the presence of different capping agents in a simple facile method producing flowerlike morphology. It is noted that the size and magnetic properties of the synthesized nickel nanoflower is guided by the choice of the capping agent. SEM studies revealed that the flowers are composed of conelike petals. The shape and size of the synthesized nickel powder is also dependent on the reaction parameters. At lower temperature (40°C), nickel with cauliflower type morphology is formed, whereas at 60°C , flowerlike nickel particles are formed. With the increase of the temperature the flowerlike morphology is destroyed and horn sphere like nickel nanoparticles are formed. Therefore, we have varied the size of the nickel nanoflower by varying the capping agent used, and we can vary the morphology by varying the temperature during the course of the reaction. The flowerlike morphology of the nickel also accounted for an enhanced coercivity and a decreased M_s value compared to that of the bulk nickel because of their size in the nanometer range. These nickel nanoflowers can be used as a catalyst due to their high specific surface area compared to the spherical nickel nanoparticles. Also, the nickel nanoflowers prepared in the presence of DEA and in the absence of any capping agent have higher remnant magnetization. Therefore, such novel and facile strategies may be further explored for the industrial scale production and application of Ni nanoparticles as effective catalysts as well as high density recording media.

Acknowledgment. S.S. is grateful to the CSIR, New Delhi, for financial support and Indian Institute of Technology Kharagpur for providing a platform for research.

References

- (1) Wu, S.-H.; Chen, D.-H. *J. Colloid Interface Sci.* **2003**, *259*, 282–286.
- (2) Majetich, S. A.; Jin, Y. *Science* **1999**, *284*, 470–473.
- (3) Zarur, A. J.; Ying, J. Y. *Nature* **2000**, *403*, 65–67.
- (4) Pilani, M.-P. *Adv. Funct. Mater.* **2001**, *11*, 323–336.
- (5) Teng, X. W.; Yang, H. *J. Am. Chem. Soc.* **2003**, *125*, 14559–14563.
- (6) Lee, K. B.; Park, S.; Mirkin, C. A. *Angew. Chem. Int. Ed.* **2004**, *43*, 3048–3050.
- (7) Arregui, M.; Galan, M.; Navascues, N.; Tellez, C.; Marquina, C.; Ibarra, M. R.; Santamaría, J. *Chem. Mater.* **2006**, *18*, 1911–1919.
- (8) Weber, A. P.; Seipenbusch, M.; Kasper, G. *J. Nanoparticle Res.* **2003**, *5*, 293–298.
- (9) Liu, Y.; Zhang, L.; Guo, Q.; Hou, H.; You, T. *Anal. Chem. Acta* **2010**, *663*, 153–157.
- (10) Al-Saleh, M. A.; Sleem-Ur-Rahman, S. M.; Kareemuddin, M. J.; Al-Zakri, A. S. *J. Power Sources* **1998**, *72*, 159–164.
- (11) Smogunov, A.; Dal Corso, A.; Tosatti, E. *Surf. Sci.* **2002**, *507*, 609–614.
- (12) Singla, M. L.; Negi, A.; Mahajan, V.; Singh, K. C.; Jain, D. V. S. *Appl. Catal. A Gen.* **2007**, *323*, 51–57.
- (13) Bai, L.; Yuan, F.; Tang, Q. *Mater. Lett.* **2008**, *62*, 2267–2270.
- (14) Liu, X.; Liang, X.; Zhang, N.; Qiu, G.; Yi, R. *Mater. Sci. Eng., B* **2006**, *132*, 272–277.
- (15) Chen, Y.; Peng, D.-L.; Lin, D.; Luo, X. *Nanotechnology* **2007**, *18*, 505703.
- (16) Green, M.; O'Brien, P. *Chem. Commun.* **2001**, 1912–1913.
- (17) Hou, Y.; Gao, S. *J. Mater. Chem.* **2003**, *13*, 1510–1512.
- (18) Chen, D. H.; Hsieh, C. H. *J. Mater. Chem.* **2002**, *12*, 2412–2415.
- (19) Chen, L.; Chen, J.; Zhou, H.; Zhang, D.; Wan, H. *Mater. Sci. Eng., A* **2007**, *452/453*, 262–266.
- (20) Jeon, Y. T.; Moon, J. Y.; Lee, G. H.; Park, J.; Chang, Y. *J. Phys. Chem. B* **2006**, *110*, 1187–1191.
- (21) Jeon, Y.; Lee, G. H.; Park, J.; Kim, B.; Chang, Y. *J. Phys. Chem. B* **2005**, *109*, 12257–12260.
- (22) Ni, X. M.; Zhao, Q. B.; Zheng, H. G.; Li, B. B.; Song, J. M.; Zhang, D. G.; Zhang, X. J. *Eur. J. Inorg. Chem.* **2005**, *23*, 4788–4793.
- (23) Ni, X.; Zhao, Q.; Zhang, D.; Zhang, X.; Zheng, H. *J. Phys. Chem. C* **2007**, *111*, 601–605.
- (24) Wang, Y.; Zhu, Q.; Zhang, H. *Mater. Res. Bull.* **2007**, *42*, 1450–1456.
- (25) Mathew, A.; Munichandraiah, N.; Rao, G. M. *Mater. Sci. Eng., B* **2009**, *158*, 7–12.
- (26) Hu, H.; Sugawara, K. *Mater. Lett.* **2009**, *63*, 940–942.
- (27) Li, Y. D.; Li, C. W.; Wang, H. R.; Li, L. Q.; Qian, Y. T. *Mater. Chem. Phys.* **1999**, *59*, 88–90.
- (28) Chen, M.; Zhou, J.; Xie, L.; Gu, G.; Wu, L. *J. Phys. Chem. C* **2007**, *111*, 11829–11835.
- (29) Grzelczak, M.; Pérez-Juste, J.; Rodríguez-González, B.; Spasova, M.; Barsukov, I.; Farle, M.; Luis, M. L.-M. *Chem. Mater.* **2008**, *20*, 5399–5405.
- (30) Li, D.; Komarneni, S. *J. Am. Ceram. Soc.* **2006**, *89*, 1510–1517.
- (31) Hegde, M. S.; Larcher, D.; Dupont, L.; Beaudoin, B.; Tekiaia-Elhsissen, K.; Tarascon, J. M. *Solid State Ionics* **1997**, *93*, 33–50.
- (32) Park, J. W.; Chae, E. H.; Kim, S. H.; Lee, J. H.; Kim, J. W.; Yoon, S. M.; Choi, J.-Y. *Mater. Chem. Phys.* **2006**, *97*, 371–378.
- (33) Li, Y. D.; Li, L. Q.; Liao, H. W.; Wang, H. R. *J. Mater. Chem.* **1999**, *9*, 2675–2677.
- (34) Guo, L.; Liu, C.; Wang, R.; Xu, H.; Wu, Z.; Yang, S. *J. Am. Chem. Soc.* **2004**, *126*, 4530–4531.
- (35) Khan, Z.; Al-Thabaiti, S. A.; El-Mossalamy, E. H.; Obaid, A. Y. *Colloids Surf., B* **2009**, *73*, 284–288.
- (36) Freund, P. L.; Spiro, M. *J. Phys. Chem.* **1985**, *89*, 1074–7.
- (37) Cheng, D.; Xia, S.; Tong, J. *Transit. Metal. Chem.* **1996**, *21*, 503–506.
- (38) Jiang, C.; Zou, G.; Zhang, W.; Yu, W.; Qian, Y. *Mater. Lett.* **2006**, *60*, 2319–2321.
- (39) Liu, Z. P.; Li, S.; Yang, Y.; Peng, S.; Hu, Z. K.; Qian, Y. T. *Adv. Mater.* **2003**, *15*, 1946–1948.
- (40) Hwang, J. H.; Dravid, V. P.; Teng, M. H.; Host, J. J.; Elliott, B. R.; Johnson, D. L.; Mason, T. O. *J. Mater. Res.* **1997**, *12*, 1076–1082.
- (41) Leslie-Pelecky, D. L.; Rieke, R. D. *Chem. Mater.* **1996**, *8*, 1770–1783.
- (42) Cao, H. O.; Xu, Z.; Sang, H.; Sheng, D.; Tie, C. Y. *Adv. Mater.* **2001**, *13*, 121–123.
- (43) Whitney, T. M.; Jiang, J. S.; Searson, P. C.; Chien, C. L. *Science* **1993**, *261*, 1316–1319.
- (44) Chen, D. H.; Wu, S. H. *Chem. Mater.* **2000**, *12*, 1354–1360.
- (45) Cordente, N.; Amiens, C.; Chaudret, B.; Respaud, M.; Senocq, F.; Casanove, M. *J. Appl. Phys.* **2003**, *94*, 6358–6365.
- (46) Shaf, K. V. P. M.; Gedanken, A.; Prozorov, R.; Balogh, J. *Chem. Mater.* **1998**, *10*, 3445–3450.
- (47) Jia, F.; Zhang, L.; Shang, X.; Yang, Y. *Adv. Mater.* **2008**, *20*, 1050–1054.
- (48) Wang, D. P.; Sun, D. B.; Yu, H. Y.; Meng, H. M. *J. Cryst. Growth* **2008**, *310*, 1195–1201.
- (49) Sahu, R. K.; Ray, A. K.; Mishra, T.; Pathak, L. C. *Cryst. Growth Des.* **2008**, *8*, 3754–3760.
- (50) Ni, X.; Zhang, Y.; Song, J.; Zheng, H. *J. Cryst. Growth* **2007**, *299*, 365–368.
- (51) Zhang, D. E.; Ni, X. M.; Zheng, H. G.; Li, T. Y.; Zhang, X. J.; Yang, Z. P. *Mater. Lett.* **2005**, *59*, 2011–2014.
- (52) Ni, X.; Zhao, Q.; Zhang, D.; Yang, D.; Zheng, H. *J. Cryst. Growth* **2005**, *280*, 217–221.